JACS
JOURNAL OF THE AMERICAN CHEMICAL SOCIETY
Article
pubs.acs.org/JACS

Full-Color Tunable Photoluminescent Ionic Liquid Crystals Based on Tripodal Pyridinium, Pyrimidinium, and Quinolinium Salts

Kana Tanabe,[†] Yuko Suzui,[‡] Miki Hasegawa,[‡] and Takashi Kato*[,†]

[†]Department of Chemistry and Biotechnology, School of Engineering, The University of Tokyo, Hongo, Bunkyo-ku, Tokyo 113-8656, Japan

[‡]Department of Chemistry and Biological Science, College of Science and Engineering, Aoyama-Gakuin Univerisity, 5-10-1 Fuchinobe, Sagamihara, Kanagawa 229-8558, Japan

Supporting Information

ABSTRACT: Color-tunable luminescent ionic liquid crystals have been designed as a new series of luminescent materials. To achieve tuning of emission colors, intramolecular charge transfer (ICT) character has been incorporated into tripodal molecules. A series of the compounds has three chromophores in each molecule, incorporated with both electron-donating moieties such as alkylaminobenzene and alkoxybenzene, and electron-accepting moieties such as pyridinium, pyrimidinium, and quinolinium parts. These C_3-symmetrical molecules self-assemble into liquid-crystalline (LC) columnar (Col) structures over wide temperature ranges through nanosegregation between ionic moieties and nonionic aliphatic chains. Photoluminescent (PL) emissions of these tripodal molecules are observed in the visible region both in the self-assembled condensed states and in solutions. For example, a pyrimidinium salt with didodecylaminobenzene moieties exhibits yellowish orange emission (λ_{em} = 586 nm in a thin film). Multicolor PL emissions are successfully achieved by simple tuning of changing electron-donating and electron-accepting moieties of the compounds, covering the visible region from blue-green to red. It has been revealed that ICT processes in the excited states and weak intermolecular interactions play important roles in the determination of the PL properties of the materials, by measurements of UV−vis absorption and emission spectra, fluorescence lifetimes, and PL quantum yields.

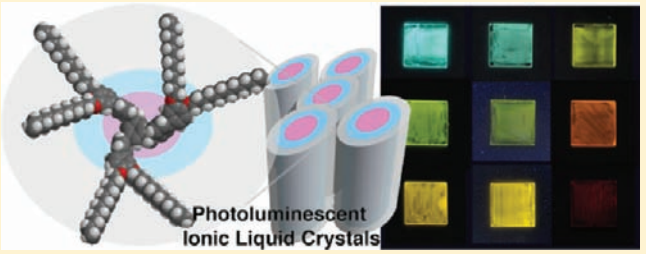

INTRODUCTION

Photoluminescence of organic compounds is a conventional, but still attractive phenomenon from the viewpoints of both fundamental science and practical applications.[1] Among a large amount of organic fluorophores including neutral and charged molecules, luminescent ionic molecules are fascinating candidates for a wide variety of applications such as sensors[2] and optoelectronic devices[3] because they have unique features such as high solubility in polar solvents, strong interfacial dipoles from the ionic moieties, possibility of ionic migration under an applied electric field, and strong molecular aggregation behavior due to the electrostatic interactions. These ionic luminescent molecules have organic aromatic chromophores. These materials are desired to exhibit luminescent properties in both solutions and solid states for various applications. Studies on the photoluminescent (PL) properties in solutions are essential for understanding the photophysics of the isolated chromophores, while those in the condensed states are necessary as well for various optoelectronic applications such as organic fluorescent sensing film,[4] organic light-emitting diodes, and organic solid-state lasers.[5] Herein, we report on new PL ionic liquid crystals exhibiting columnar liquid-crystalline (LC) states. The basic molecular design is push−pull type C_3-symmetrical ions bearing long alkyl chains (Figure 1). To date, color-tunable emissions have not been obtained for ionic liquid crystals in bulk states.

However, emissions from organic chromophores are usually suppressed in their condensed states even if they are highly emissive in solutions. This general phenomenon occurs due to the concentration quenching caused by intermolecular interactions such as energy transfer and excimer formation. In some cases, opposite phenomena are observed in which chromophores are more emissive in the aggregated states than in the solutions. This behavior is called as aggregation-induced emission (AIE) or aggregation-induced emission enhancement (AIEE), which is often explained by the restriction of the molecular motion in the aggregated states.[6] "Aggregated states" represent various bulk states with no solvent such as powder, thin films, single crystals, and liquid crystals as well as aggregation in solutions. Among them, liquid crystals are quite attractive materials because they have both liquid-like fluidity and crystal-like order and have a wide variety of applications such as electric and optical functional devices.[7,8]

Ionic liquid crystals have attracted much attention[9] because of their potential to act as organized reaction media, anisotropic

Received: January 8, 2012
Published: February 28, 2012

   dx.doi.org/10.1021/ja3001979 | J. Am. Chem. Soc. 2012, 134, 5652−5661

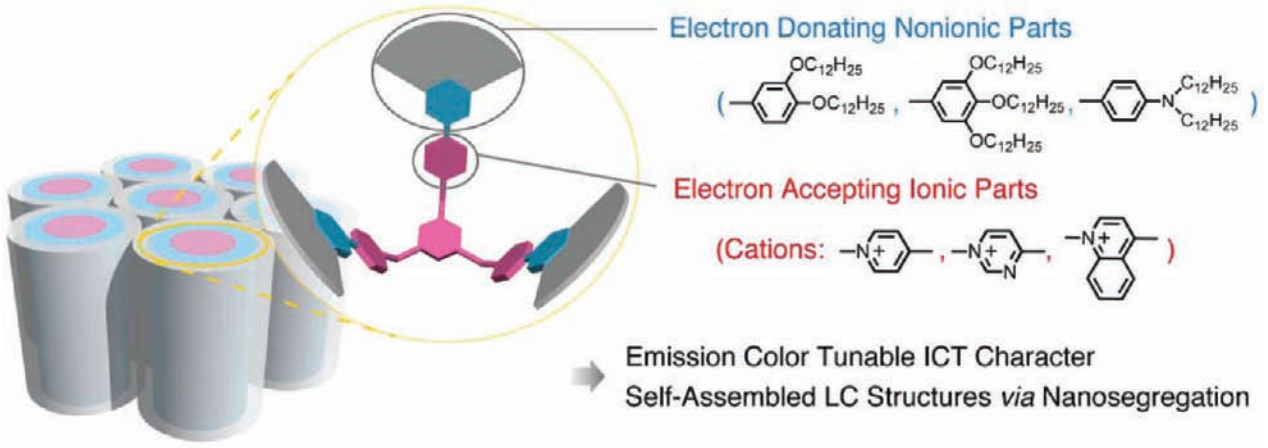

Figure 1. Schematic illustrations of molecular design.

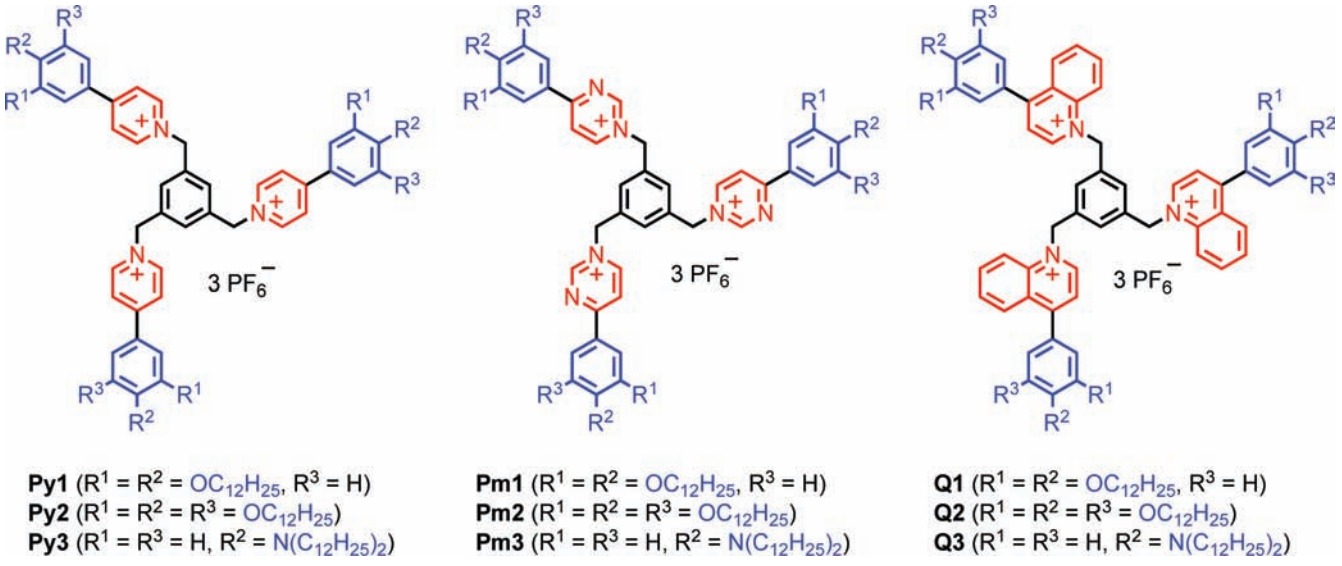

Figure 2. Molecular structures of tripodal pyridinium salts **Py1**−**3**, pyrimidinium salts **Pm1**−**3**, and quinolinium salts **Q1**−**3**.

ion-conductive materials,[10] and redox-active materials.[11] Despite their potential applications, there are only a few PL ionic liquid crystals reported such as pyrilium,[12] oxadiazolylpyridinium,[13] benzobis(imidazolium),[14] and pyrazolium salts.[15] Recently, Ziessel and co-workers have prepared highly luminescent ionic liquid crystals based on BODIPY and anthracene cores.[16] The limited number of luminescent ionic liquid crystals is partially due to the smallness of the π-conjugation of ionic LC molecules. Moreover, their small π-conjugation restricts the variety of the emission color. Hence, sufficient insight has not yet been obtained either on the fundamental properties or on the applications. The development of the methodology for the design on the LC molecules based on simpler luminescent ionic cores would enable us to gain the insight into the photophysical properties of ionic compounds not only as isolated molecules but also as self-assembled LC materials, leading to the development of a new series of color-tunable luminescent materials.

To obtain multicolor fluorescence from small π-conjugated moieties, it is a useful approach to attach both electron-donating and -accepting parts to the ends of a chromophore. Such donor (D)−acceptor (A) type chromophores can exhibit photoinduced fluorescence emission via the excited-state intramolecular charge transfer (ICT) reactions. It is well-known that aminobenzonitrile derivatives in polar solvents show dual fluorescence, which originates from locally excited and twisted ICT (TICT) states.[17] Not only such neutral D−A molecules, but also an ionic D−A system can exhibit such fluorescence from an excited ICT state. For example, Fromherz et al. have reported that the emission from excited TICT state of aminophenyl pyridinium salts is observed in polar solutions.[18] To date, however, most of the study on the emission of such ionic D−A compounds has been conducted in solutions, not in the self-assembled condensed states. Here, we report on the self-assembled structures and the photophysical properties of tripodal ionic LC compounds.

In this context, cationic organic compounds **Py1**−**3**, **Pm1**−**3**, and **Q1**−**3** were designed (Figure 2). In our molecular design, each of three kinds of electron donating dodecyloxy- or dodecylaminophenyl groups is attached to each of three kinds of electron-accepting cationic parts. As electron-donating parts, 3,4-didodecyloxybenzene (for compounds **Py1**, **Pm1**, and **Q1**), 3,4,5-tridodecyloxybenzene (for compounds **Py2**, **Pm2**, and **Q2**), or 4-(*N*,*N*-didodecylamino)benzene moieties (for compounds **Py3**, **Pm3**, and **Q3**) are introduced at three terminals of the tripodal molecules. For electron-accepting parts, pyridinium

dx.doi.org/10.1021/ja3001979 | J. Am. Chem. Soc. 2012, 134, 5652−5661

Scheme 1. Synthetic Routes of Tripodal Pyridinium, Pyrimidinium, and Quinolinium Salts

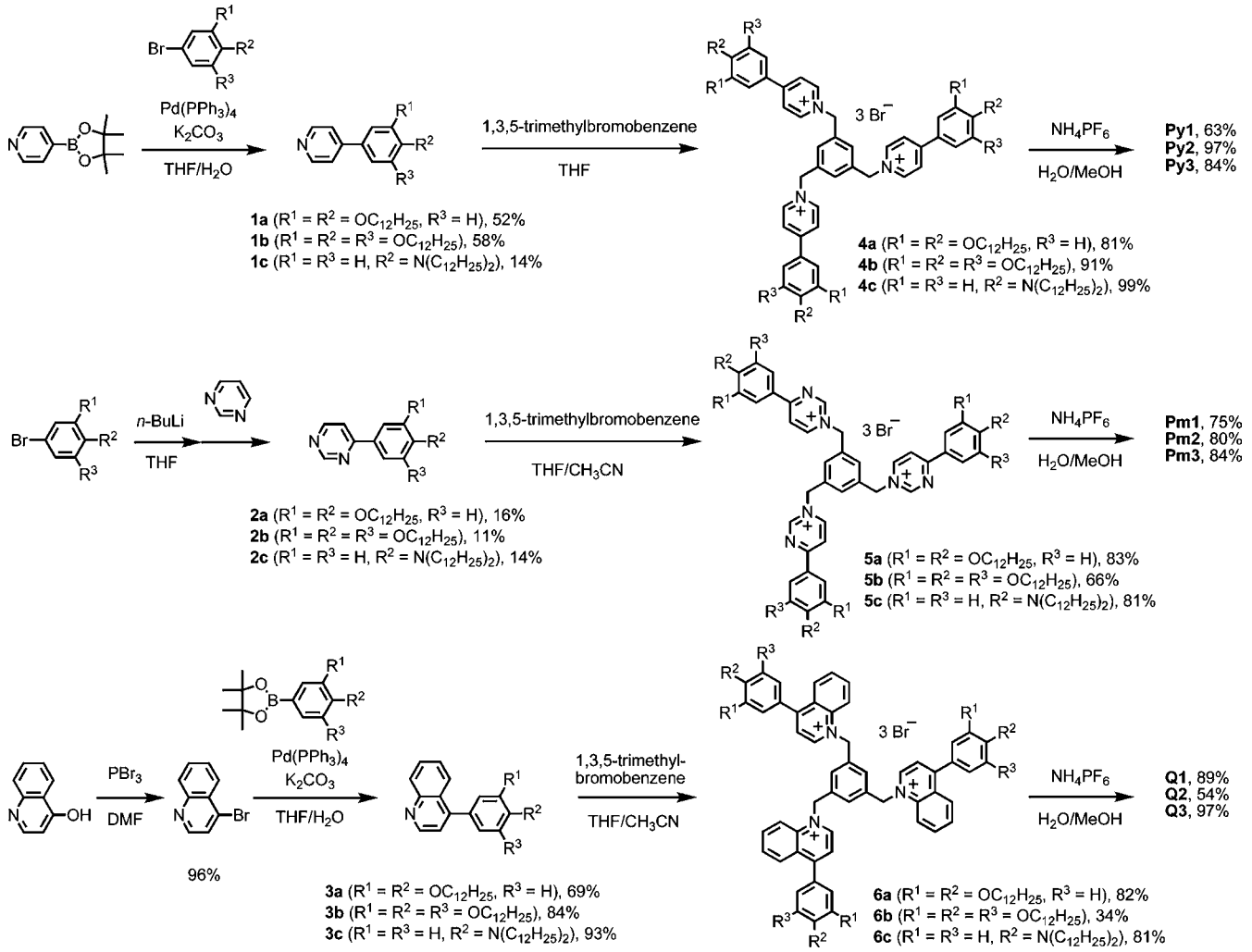

salts (for compounds **Py1**−**3**), pyrimidinium salts (for compounds **Pm1**−**3**), or quinolinium salts (for compounds **Q1**−**3**) are incorporated with these compounds. Terminal long alkyl chains are expected to enhance the nanosegregation between ionic and nonionic parts, which lead to the formation of self-assembled LC structures. As an entire molecular shape, tripodal shape is employed for all of the compounds, which would be of advantage to chemoselective molecular and anion recognition,[19] leading to the possibility of applications for sensory materials. In our preliminary communication, thermal properties and photophysical properties was reported only for pyridinium salt **Py2**.[20] C_3-symmetrical molecular shape[21] would facilitate the formation of self-assembled columnar structures that can be easily aligned, leading to one-dimensional carrier transport[10] and polarized photoluminescence.[22]

RESULTS AND DISCUSSION

Syntheses of the Tripodal Salts. All of the tripodal compounds were prepared by quaternization reactions of the corresponding phenylpyridine, phenylpyrimidine, or phenylquinoline derivatives with 1,3,5-tribromomethylbenzene followed by the counteranion exchange from bromide to hexafuluorophosphate in moderate or high yields (Scheme 1, see Supporting Information in details). All of the compounds were characterized by ^{1}H and ^{13}C NMR spectroscopy, elemental analysis, and MALDI-TOF mass spectroscopy.

Liquid-Crystalline Properties. All of the compounds exhibit LC columnar phases (Figure 3, Table 1). The self-assembled structures of these tripodal compounds were studied by differential scanning calorimetry (DSC) and X-ray diffraction (XRD) measurements. Compound **Py1** shows a crystal (Cryst)−rectangular columnar (Col_r) phase transition at

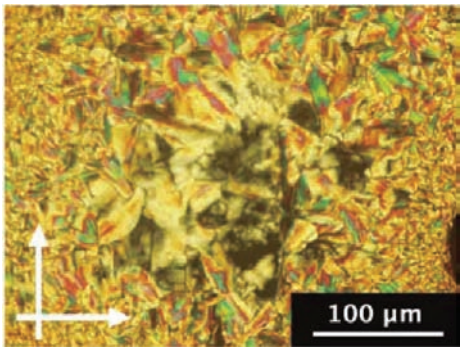

Figure 3. Polarized optical micrograph of the tripodal pyridinium salt **Py1** at 235 °C in the Col phase. Arrows indicate the directions of polarizer and analyzer axes.

dx.doi.org/10.1021/ja3001979 | J. Am. Chem. Soc. 2012, 134, 5652−5661

Table 1. Thermal Properties of the Tripodal Salts

compound	phase transition behavior[a]	lattice parameters
Py1	Cryst 48 (14) Col_r 120 (19) Col 240[b] Iso	a = 74.0 Å, b = 34.5 Å (Col_r)[c]
Py2	$Cryst_1$ 13 (6) $Cryst_2$ 24 (7) Col_r 245[b] Iso	a = 77.4 Å, b = 33.4 Å (Col_r)[d]
Py3	Cryst −30 (0.4) Col_r 105 (4) Cub 180[b] Iso	a = 73.1 Å, b = 35.7 Å (Col_r)[e]
Pm1	Cryst 86 (19) Col_r 210[b] Iso	a = 76.4 Å, b = 42.3 Å (Col_r)[f]
Pm2	Cryst −32 (25) Col_r 240[b] Iso	a = 73.4 Å, b = 29.1 Å (Col_r)[d]
Pm3	Glassy −10 Col_h 176 (0.8) Iso	a = 40.9 Å (Col_h)[d]
Q1	Cryst 56 (11) Col_r 191 (2) Iso	a = 81.0 Å, b = 41.7 Å (Col_r)[g]
Q2	Cryst −37 (26) Col_h 223 (3) Iso	a = 42.9 Å (Col_h)[h]
Q3	Glassy 79 (0.3) Col_h 210[b] Iso	a = 42.1 Å (Col_h)[i]

[a]Transition temperatures and enthalpies (kJ mol^{-1}, in parentheses) were determined by DSC measurements on the second heating at 10 °C min^{-1}. Cryst, crystalline; Glassy, glassy; Col_h, hexagonal columnar; Col_r, rectangular columnar; Col, unidentified columnar; Cub, unidentified cubic; Iso, isotropic; dec., decomposition. [b]The transition temperatures were determined by polarizing optical microscope. [c]Measured at 80 °C. [d]Measured at 140 °C. [e]Measured at 50 °C. [f]Measured at 180 °C. [g]Measured at 160 °C. [h]Measured at 90 °C. [i]Measured at 100 °C.

48 °C. In the formation of LC columnar structures, segregation between ionic pyridinium units and nonionic aliphatic parts could be an important driving force in a way similar to previously reported ionic liquid crystals (Figure 4).[9−11] When the number of the alkoxy chains is increased from six to nine, the melting temperatures are decreased. For example, the melting temperature of compound **Py2** with nine terminal dodecyloxy chains (T_m = 24 °C) is lower than that of compound **Py1** with six terminal dodecyloxy chains (T_m = 48 °C). As the number of alkoxy chains increases, central ionic cores become more surrounded by the flexible aliphatic moieties, which would lead to the stabilization of the LC columnar structures. As the temperature rises above 240 °C, all of the compounds gradually start to exhibit phase transitions to isotropic liquids or to decompose before reaching the isotropization temperatures with disappearance of the optical textures, which does not recover after the thermal decomposition.

The preferable self-assembled structures are changed from Col_r to hexagonal columnar (Col_h) structures via a structural change of ionic cores such as expansion of the hetero rings (i.e., quinolinium salts) and the introduction of nitrogen atoms (i.e., pyrimidinium salts). All three pyridinium salts **Py1−3** form Col_r phases, while pyrimidinium salts **Pm3** and quinolinium salts **Q2** and **Q3** form Col_h structures. For example, Figure 5

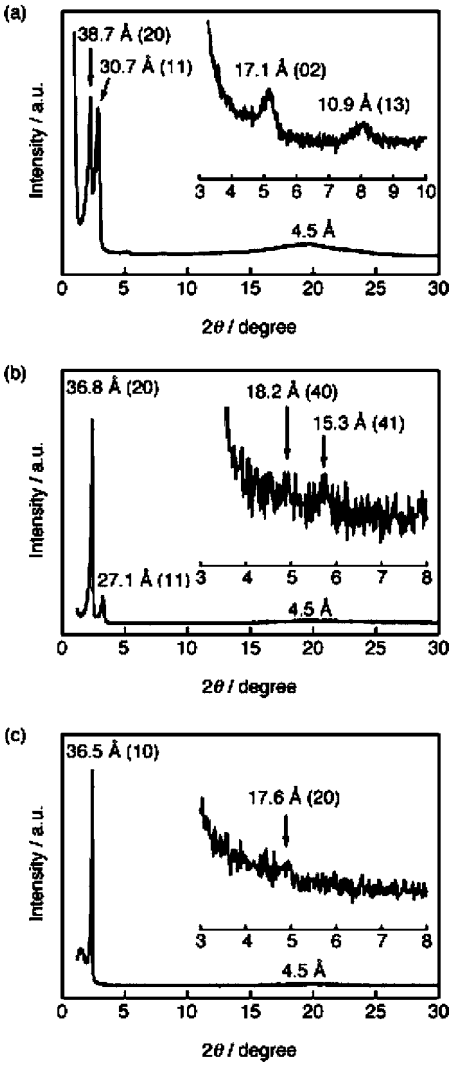

Figure 5. X-ray diffraction patterns of the tripodal salts (a) **Py2**, (b) **Pm2**, and (c) **Q2** at 140 °C in the Col phases.

shows the XRD patterns of compounds **Py2**, **Pm2**, and **Q2** measured at 140 °C. The XRD pattern of pyridinium salt **Py2** shows two intense peaks at 38.7 and 30.7 Å and two weak peaks at 17.1 and 10.9 Å, which are assigned to the (20), (11), (02), and (13) reflections of a rectangular lattice with the lattice parameters of a = 77.4 Å and b = 33.4 Å (Figure 5a). Pyrimidinium salt **Pm2** exhibits analogous XRD patterns (Figure 5b), suggesting that **Pm2** self-assembles into Col_r structures in a manner similar to **Py2**. Meanwhile, the XRD pattern of quinolinium salt **Q2** shows only one intense peak at

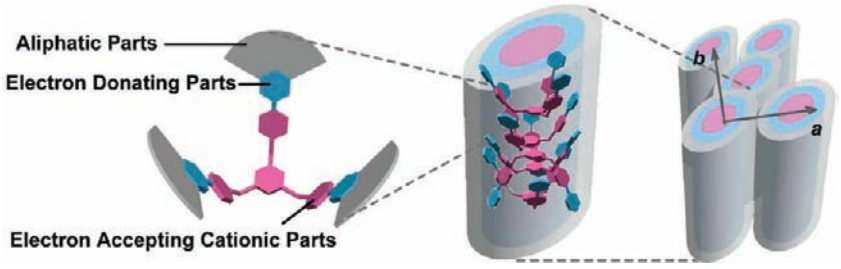

Figure 4. A schematic representation of the self-assembled columnar structure of tripodal salts. PF_6 anions are omitted for clarity.

dx.doi.org/10.1021/ja3001979 | J. Am. Chem. Soc. 2012, 134, 5652−5661

36.5 Å and a weak peak at 17.6 Å. In conjunction with a fan texture in POM image of **Q2**, characteristic of a columnar phase, these peaks can be assigned to the (10) and (20) reflections of a hexagonal columnar structure (Figure 5c, Supporting Information). This behavior can be explained by the flexibility of the three arms of tripodal molecules. As the ionic cores become larger, intramolecular rotation of the arms may become restricted due to steric repulsions between ionic cores. In a similar way, the introduction of nitrogen atoms can lead the restriction of the intramolecuar rotation due to the electrostatic repulsion between the lone pair of nitrogen atom and the closest π-electron systems. Only a little rotational flexibility of tripodal molecules can lead to comparatively circular molecular shape. Such molecules would stack along their perpendicular axises, leading to columnar structures that self-assemble into hexagonal order.

Photophysical Properties in the Condensed States. As shown in Figure 6, all of the compounds exhibit PL emissions

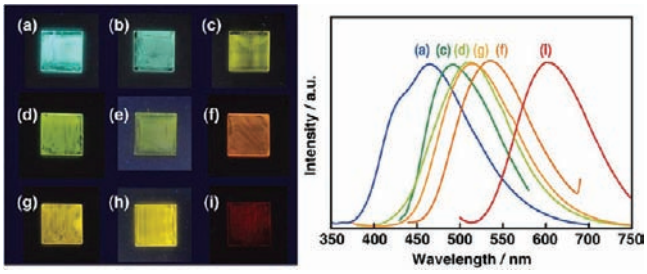

Figure 6. Photographs (left) and selected photoluminescence spectra (right) of the tripodal compounds (a) **Py1**, (b) **Py2**, (c) **Py3**, (d) **Pm1**, (e) **Pm2**, (f) **Pm3**, (g) **Q1**, (h) **Q2**, and (i) **Q3** in the condensed states. These photographs were taken under UV light (365 nm) irradiation in the bulk states at room temperature.

in their LC or solid states. It is noteworthy that the emission colors in this series cover the visible region from blue to red even in their condensed states. This is the first example of the series of PL ionic liquid crystals that show multicolored luminescence. Details in photophysical properties of the compounds are shown in Table 2.

Fluorescence quantum yields (Φ_f) for these compounds in annealed films were determined with an absolute PL quantum yield measurement system (see Experimental Section for details). For pyridinium salts **Py1**−**3**, the values of Φ_f in the thin films are much lower than those in the chloroform solutions. For example, Φ_f of **Py1** in the condensed state is 0.116, while that in dichloromethane solution is 0.414. It is a common phenomenon that the formation of delocalized excitons in the condensed states quenches the emission of organic lumminophores.[1] In contrast, the bulk states of pyrimidinium **Pm1**−**3** and quinolinium salt **Q1**−**3** are more emissive than the solution states except for **Pm2**. In particular, Φ_f values of quinolinium salts **Q1**−**3** are about 10−20 times larger than those in solutions. For example, **Q2** is emissive in the LC state with the Φ_f of 0.088, while it is nearly nonemissive in the solution (Φ_f = 0.004). The enhanced emission is ascribed to the aggregation-induced emission enhancement (AIEE).[6] Although the origin of this AIEE phenomenon is not fully understood, aggregation-induced restriction of the molecular motion or planarization of the distorted chromophore units may occur as Tang et al. have explained on the AIE or AIEE behavior of pentaphenylsilole and biphenyl derivatives.[6] In the present study, the rotation between cationic heteroring and electron-donating phenyl ring could be restricted or slow down when the molecules assemble with each other. In the case of quinolinium salts **Q1**−**3**, due to the steric hindrance of three quinoline rings of the tripodal molecules, chromophores could not assemble into close-packing structures even in the condensed states, whereas pyridinium salts **Py1**−**3** and pyrimidinium salts **Pm1**−**3** have relatively large spaces at the center of the molecules. As a result, photoluminescence from only **Q1**−**3** is significantly enhanced in the condensed states. In addition, these PL wavelengths are not definitely changed by the thermal phase transitions between Cryst and LC phases. For example, compound **Py1** shows bluish green photoluminescence with a peak at 515 nm in the Cryst phase at room temperature, and at 512 nm in the Col phase at 100 °C (Figure 7). Only a little change of the peak positions is observed upon the Cryst−Col phase transition. This behavior indicates that interactions between the cationic chromophores of the tripodal salts are not affected by the self-assembled structures.

Photophysical Properties in Solution. All of the tripodal compounds exhibit fluorescence emission both in solution as well as in the condensed states (Table 2). For example, pyridinium salt **Py1** shows blue-green emission in the dichloromethane solution with the absorption maximum at 386 nm and the emission maximum at 511 nm. This emission may originate from the ICT excited state, due to that the

Table 2. Photophysical Properties of the Tripodal Salts[a]

	in solution					in annealed films[b]			
compound	λ_{abs}[c]/nm	λ_{em}[d]/nm	Stokes shift/eV	E_g/eV	Φ_f[e]	λ_{abs}/nm	λ_{em}/nm	Φ_f	state
Py1	386	511	0.79	2.76	0.414	380	515	0.116	Cryst
Py2	375	518	0.91	2.74	0.153	375	520	0.043	Col_r
Py3	463	530	0.34	2.39	0.152	432	542	0.048	Col_r
Pm1	414	526	0.64	2.59	0.064	399	560	0.093	Cryst
Pm2	408	524	0.67	2.58	0.026	388	578	0.011	Col_r
Pm3	494	535	0.19	2.30	0.021	465	586	0.037	Col_h
Q1	323, 425	598	0.84	2.38	0.012	323, 408	563	0.126	Cryst
Q2	321, 409	608	0.99	2.51	0.004	322, 391	577	0.088	Col_h
Q3	288, 533	651	0.42	2.00	0.005	286, 506	652	0.042	Glassy

[a] λ_{abs}, absorption maxima; λ_{em}, emission maxima; E_g, HOMO−LUMO gaps estimated from the onset positions of the UV−vis absortption spectra; Φ_f, fluorescence quantumn yields.; Cryst, crystalline; Glassy, glassy; Col_h, hexagonal columnar; Col_r, rectangular columnar. Excitation wavelengths are consistent with λ_{abs} of the same samples. [b] Annealed at 180 °C for 10 min and then cooled to room temperature. Measured at room temperature. [c] Measured in 1.0×10^{-5} M dichloromethane solutions. [d] Measured in 1.0×10^{-6} M dichloromethane solutions. [e] Measured in chloroform solutions.

dx.doi.org/10.1021/ja3001979 | J. Am. Chem. Soc. 2012, 134, 5652−5661

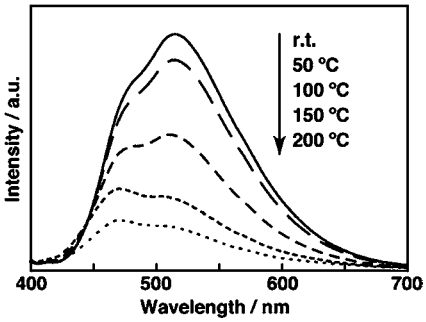

Figure 7. Photoluminescence spaectra of **Py1** in the Cryst phase at room temperature and in the Col phase at 50, 100, 150, and 200 °C. The excitation wavelength is 380 nm.

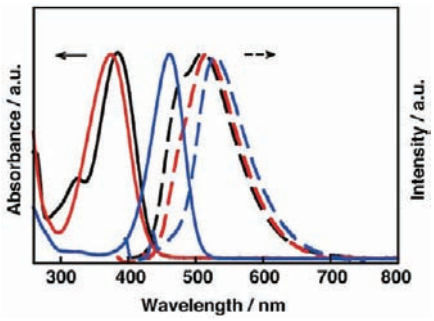

Figure 9. Normalized absorption (solid lines) and photoluminescence spectra (dashed lines) of the pyridinium salts **Py1** (indicated in black), **Py2** (red), and **Py3** (blue) in dichloromethane solutions.

structures of the chromophores have both electron donor and acceptor substituents. To confirm the ICT character of the tripodal molecule, frontier molecular orbitals have been studied by density functional theory (DFT) calculations for the model compound. Figure 8 shows the highest occupied molecular orbital (HOMO), second HOMO (HOMO−1), and lowest unoccupied molecular orbital (LUMO) of the model compound for **Py1** with shorter alkyl chains. HOMO and HOMO−1 localize the electron-donating dialkoxy benzene units, while LUMO localizes the electron-accepting pyridinium parts, and the three chromophores are independent from each other. Compound **Py1** with longer alkyl chains may have analogical electronic structure, which would lead to the ICT feature of the molecule. To study the origin of the ICT emission in detail, substituent and solvent effects were studied (vide infra).

Effects of Electron-Donating Parts on the Photophysical Properties. To examine the effects of electron-donating moieties on the photophysical properties, the electronic properties of electron-donating parts are directly compared in the single core skeleton. In the single skeleton, the electron-donating abilities are considered to be increased in the following order: 3,4-didodecyloxybenzene (electron-donating parts for compounds **Py1**, **Pm1**, and **Q1**), 3,4,5-tridodecyloxybenzene (for **Py2**, **Pm2**, and **Q2**), and 4-(*N*,*N*-didodecylamino)benzene (for **Py3**, **Pm3**, and **Q3**). For representative examples, absorption and emission spectra of pyridinium salts **Py1**−**3** are given in Figure 9. On the core skeleton with pyridinium salts (compounds **Py1**−**3**), the corresponding wavelengths of absorption maxima are 386, 375, and 463 nm in dichloromethane solutions, respectively. The bathochlomic shift of absorption wavelength is obtained in the order of **Py2**, **Py1**, and **Py3**. On the other single skeleton, the same tendency is observed, where 3,4-didodecyloxybenzene (for **Py1**, **Pm1**, and **Q1**) induces more bathochromic shift in the absorption wavelength than expected from the number of alkoxy chains. This tendency can be explained by the asymmetrical structure of 3,4-didodecyloxybenzene in the single chromophore; however, details are under investigation. In the PL spectra of compounds **Py1**−**3**, the wavelength of emission maxima are 511, 518, and 530 nm, respectively. In addition, the values of the Stokes shift are decreased in the order of **Py2**, **Py1**, and **Py3**.

Frontier molecular orbitals have been studied by DFT calculations for the model monocationic compounds with shorter alkyl chains (Figure 10). For the model compounds of **Py1** and **Py2** having alkoxy chains as their electron-donating groups, the HOMO orbitals are located on the electron-donating groups, whereas the LUMO orbitals are localized on the electron-accepting cationic parts. These orbitals are considered as largely π orbitals of the electron-donating alkoxyphenyl groups and π^* orbitals of the electron-accepting pyridinium units, respectively. For the model compound of **Py3** having an alkylamino group, the HOMO is comparatively delocalized all over the cationic chromophore, which is explained by an involvement of the lone electron pair on the

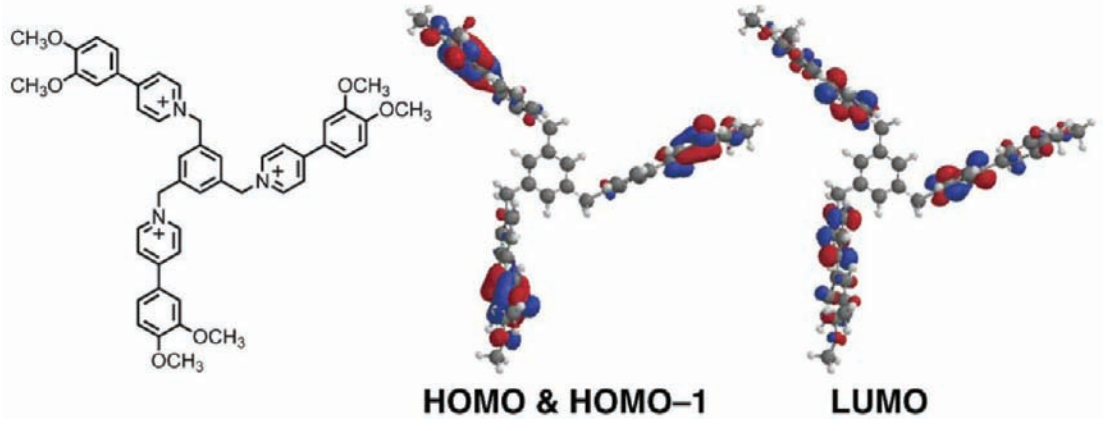

Figure 8. Molecular structure of the model tripodal compound for pyridinium salt **Py1** and representation of the frontier orbitals (HOMO, HOMO−1, and LUMO) of the model compounds obtained from DFT calculations at the B3LYP/6-31G* level.

dx.doi.org/10.1021/ja3001979 | *J. Am. Chem. Soc.* 2012, 134, 5652−5661

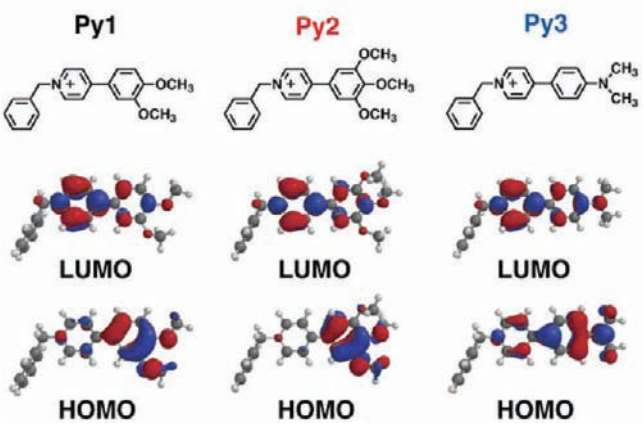

Figure 10. Representation of the frontier orbitals of the model compounds for pyridinium salts **Py1**−**3** obtained from DFT calculations at the B3LYP/6-31G* level. Molecular structures of the model compounds are indicated on the top of the figure. Upper orbitals indicate LUMOs, and the bottom orbitals indicate HOMOs for the model compounds.

nitrogen atom of the dialkylamino group in the conjugation of the phenylpyridine backbone. As a result of this elongation of conjugation, increase in the absorption and emission maxima might be obtained for the alkylaminobenzene derivative **Py3** as compared to the corresponding alkoxybenzene derivatives **Py1** and **Py2**.

Effects of Electron-Accepting Parts on the Photophysical Properties. The direct comparison of the electronic properties of electron-accepting moieties is conducted as well as electron-donating parts. Figure 11 shows the absorption and

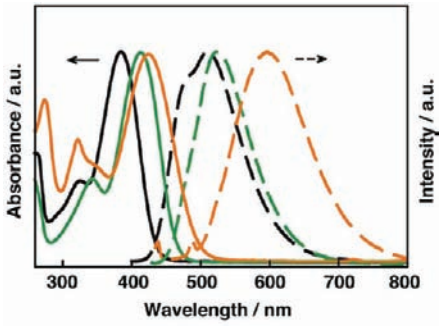

Figure 11. Normalized absorption (solid lines) and photoluminescence spectra (dashed lines) of the pyridinium salts **Py1** (indicated in black), **Pm1** (green), and **Q1** (orange) in dichloromethane solutions.

emission spectra of compounds **Py1**, **Pm1**, and **Q1** having 3,5-didodecylaminobenzene as the single electron donating part. Both for pyrimidinium salt **Pm1** and quinolinium salt **Q1**, the absorption maxima are red-shifted as compared to those of corresponding pyridinium salt **Py1** by 28 and 39 nm, respectively (λ_{abs} = 386 nm for **Py1**; λ_{abs} = 414 nm for **Pm1**; λ_{abs} = 425 nm for **Q1**). The same tendency is observed in the emission maxima (λ_{em} = 511 nm for **Py1**; λ_{em} = 526 nm for **Pm1**; λ_{abs} = 598 nm for **Q1**). This is attributed to more electron-deficient property of pyrimidine ring and π-expanded nature of quinoline ring as compared to pyridine ring, either of which results in low-lying LUMO level, leading to red-shifted absorption and emission. Figure 12 depicts frontier orbitals of the model monocationic compounds for **Py1**, **Pm1**, and **Q1**.

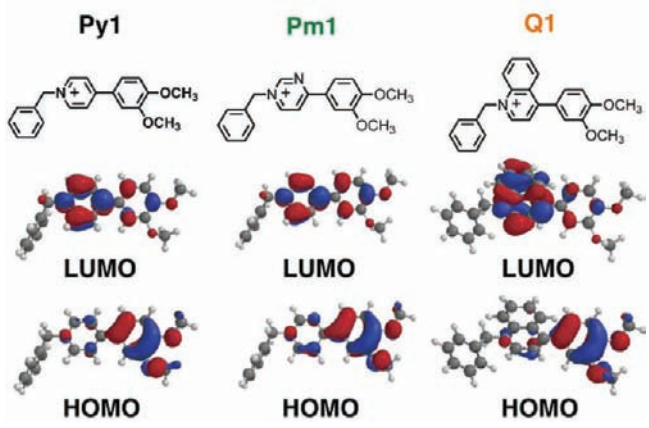

Figure 12. Representation of the frontier orbitals of the model compounds for compounds **Py1**, **Pm1**, and **Q1** obtained from DFT calculations at the B3LYP/6-31G* level. Molecular structures of the model compounds are indicated on the top of the figure. Upper orbitals indicate LUMOs, and the bottom orbitals indicate HOMOs for the model compounds.

For all of the compounds, the HOMOs are almost totally localized on the electron-donating dialkoxybenzene moieties, while the LUMOs are mainly localized on the electron-accepting cationic parts, in a manner similar to the discussion on the effect of electron-donating nature.

Solvent Effects on the Photophysical Properties. To study the CT character of the tripodal salts, solvent effects on the PL properties were studied. For example, the results of pyridinium salts **Py1**−**3** are shown below. Photoluminescence spectra were measured in different solvents with various polarities (see the Supporting Information). All of the compounds show obvious positive solvatochromism in the PL spectra except for cyclohexane solutions, where the molecules are considered to aggregate with each other because the solvent polarity is too low to disperse such ionic molecules. This behavior is illustrated more clearly in Figure 13 where the emission maxima (ν_{max}, in wavenumber) are plotted against the solvent polarity parameter $E_T(30)$.[23] For all of the compounds, ν_{max} values decrease with increasing solvent polarity, obeying close-to-linear relationship for $E_T(30)$ values. Moreover, relatively large Stokes shifts (0.4−2.2 eV) and a lack of fine structure emission of the tripodal compounds also indicate the

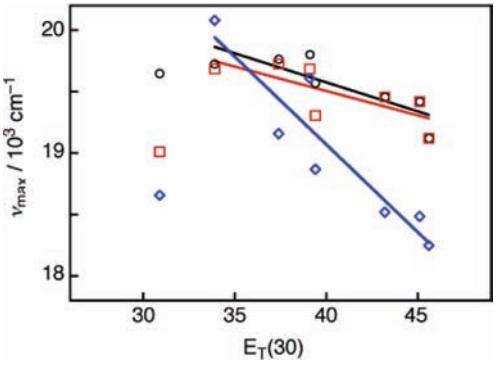

Figure 13. The dependence of the emission maxima for compounds **Py1** (indicated in black), **Py2** (red), and **Py3** (blue) on the solvent polarity parameter $E_T(30)$. The data recorded in cyclohexane are omitted for linear regression analyses due to low solubility of the compounds.

dx.doi.org/10.1021/ja3001979 | J. Am. Chem. Soc. 2012, 134, 5652−5661

Table 3. Fluorescence Lifetimes of the Pyridinium Salts Py1−3 in Thin Films

		as-spin-coated film[a]					annealed film[b]				
compound	λ_{em}/nm	τ_1/ns	τ_2/ns	A_1	A_2	χ	τ_1/ns	τ_2/ns	A_1	A_2	χ
Py1	385−470	4.3	15.4	0.94	0.06	1.005	<2	6.9	0.97	0.03	1.018
	450−588	4.0	11.9	0.83	0.17	1.121	4.1	12.5	0.95	0.05	1.051
	550−650	6.9	19.3	0.88	0.12	1.166	5.9	23.3	0.95	0.05	0.991
Py2	455−593	6.5	16.1	0.95	0.05	1.022	2.9	8.7	0.91	0.09	0.999
Py3	477−615	2.7	11.9	0.95	0.05	1.144	3.7	17.3	0.98	0.02	1.040

[a]Spin-coated from chloroform solutions. [b]Annealed at 180 °C for 10 min and then cooled to room temperature.

strong ICT character of the chromophores. This indicates efficient charge shifts in the excited states of these compounds, which are compatible with the frontier orbital pictures of the model monocationic compounds obtained through DFT calculations as mentioned above.

Fluorescence Lifetime Measurements. To study the origin of the PL emissions, the fluorescence lifetimes for the tripodal salts were measured both in solutions and in the condensed states. In chloroform solutions, it was revealed that these compounds have two PL components with lifetimes of nanosecond order. For example, compound **Py1** has two PL components with lifetimes of ca. 1 and 5 ns. Fluorescence lifetime measurements in the condensed states were also conducted for both as-spin-coated films and annealed spin-coated films.

For the as-spin-coated films in which tripodal molecules are rather randomly assembled with each other with electrostatic interactions and van der Waals interactions, two emissive components have been observed with mostly slower lifetimes than those in solutions. As shown in Table 3, all of the molecules decay through two relaxation pathways. For example, the lifetimes of compound **Py1** in an as-spincoated film are revealed to be 4 ns (83%) and 12 ns (17%) at emission wavelength in the range of 450−588 nm. Two emissive components are observed even in the films, both of which can be attributed to monomeric components from intramolecular CT states. The shorter ones can be assigned to be the emissive components with little perturbation and the longer ones to be those without obvious intermolecular interactions (see also the Supporting Information). Their vibrational deactivation pathways are preferably suppressed in the as-spin-coated films because of the restriction of the intramolecular vibrational and rotational motions.

As compared to the as-spin-coated films, it was revealed that the origin of emissions places a disproportionate emphasis on the shorter components of the two in the annealed films. For example, compound **Py1** in an annealed film has two pathways with lifetimes of 4 ns (95%) and 13 ns (5%) at emission wavelength in the range of 450−588 nm, which are much more dominated by the former component than those in the spin-coated films mentioned above. This indicates that annealing of the films may lead to closer packing of the self-assembled molecules having interactions with each other, which results in the existence of larger amounts of molecules with a fast process of radiative decay.

CONCLUSION

We have demonstrated LC materials with simple ionic cores, which show full-color tunable emission ranging over the visible region simply by changing electron-donating and -accepting abilities. These LC materials are a new series of tripod-shaped pyridinium, pyrimidinium, and quinolinium salts, which self-organize into columnar or micellar cubic LC phases via nanosegregation between ionic and nonionic moieties. Our finding in the present study gives us new insights into fundamental research for the luminescent compounds on molecular conformation, intramolecular motion, and intermolecular interactions in the self-assembled condensed states. Moreover, the results can be useful for materials design for potential applications such as organic fluorescent sensors and optoelectronic materials.

EXPERIMENTAL SECTION

General. ^{1}H and ^{13}C{^{1}H} NMR spectra were recorded on a JEOL JNM-LA400 spectrometer. Mass spectra were obtained with a PerSeptive Biosystems Voyager-DE STR spectrometer. Elemental analyses were carried out with a Yanaco MT-6 CHN autocorder.

Thermal properties of compounds **Py1−3**, **Pm1−3**, and **Q1−3** were examined by polarizing optical micrography (POM), differential scanning calorimetry (DSC), and X-ray diffraction (XRD) measurements. DSC measurements were performed on a NETZSCH DSC204 Phoenix calorimeter at a scanning rate of 10 °C min^{-1}. A POM Olympus BH-51 equipped with Linkam LTS 350 hot stage was used for visual observation. XRD patterns were obtained using a Rigaku RINT-2500 diffractometer with a heating stage using Ni-filtered Cu Kα radiation. UV−vis absorption and photoluminescence spectra were measured with JASCO V-670 and a JASCO FP-777W spectrometers, respectively. The excitation wavelength used was that of the UV−vis absorption maximum of each sample. The fluorescence quantum yield (Φ_f) was measured with an absolute PL quantum yield measurement system (Hamamatsu C9920-02), in which excitation was provided with a Xe lamp after passing through a monochromator.[24] The fluorescence lifetime was measured with HAMAMATSU C4334 streak scope.

Materials and Syntheses. All reagents and solvents were purchased from Aldrich, Tokyo Kasei, Kanto Chemical, or Wako, and used as received. The synthetic routes used to obtain pyridinium salts (**Py1−3**), pyrimidinium salts (**Pm1−3**), quinolinium salts (**Q1−3**) are shown in Scheme 1. 4-Bromoquinoline,[25] 1-bromo-3,4-didodecyloxybenzene,[26] 1-bromo-3,4,5-tridodecyloxybenzene,[20] 4-(3,4,5-didodecyloxyphenyl)pyridine (**1b**),[20] 1,3,5-tris(4-(3,4,5-tridodecyloxyphenyl)pyridiniummethyl)benzene bromide (**4b**),[20] and 1,3,5-tris(4-(3,4,5-tridodecyloxyphenyl)pyridiniummethyl)benzene hexafluorophosphate (**Py2**)[20] were prepared according to the literature. For other compounds, details in the syntheses and characterization data are included in the Supporting Information.

ASSOCIATED CONTENT

Supporting Information

Syntheses and characterization of compounds **Py1**, **Py3**, **Pm1−3**, **Q1−3**, **1a**, **1c**, **2a−c**, **3a−c**, **4a**, **4c**, **5a−c**, and **6a−c**, and additioncal photophysical properties of the compounds. This material is available free of charge via the Internet at http://pubs.acs.org.

AUTHOR INFORMATION

Corresponding Author

kato@chiral.t.u-tokyo.ac.jp

Notes

The authors declare no competing financial interest.

ACKNOWLEDGMENTS

We thank Mr. Daisuke Kodama for the measurements of fluorescence quantum yield and lifetime of a reference compound. This work was partially supported by a Grant-in-Aid for Scientific Research (A) (no. 19205017) from the Japan Society for the Promotion of Science (JSPS) and a Grant-in-Aid for a Scientific Research on Innovative Areas of "Fusion Materials: Creative Development of Materials and Exploration of Their Function through Molecular Control" (area no. 2206) and the Global COE Program for Chemistry Innovation from the Ministry of Education, Culture, Sports, Science, and Technology. K.T. is grateful for financial support from the JSPS Research Fellowship for Young Scientists.

REFERENCES

(1) *Molecular Fluorescence: Principles and Applications*; Valeur, B., Ed.; Wiley-VCH: Weinheim, 2001.

(2) (a) Ho, H.-A.; Boissinot, M.; Bergeron, M. G.; Corbeil, G.; Doré, K.; Boudreau, D.; Leclerc, M. *Angew. Chem., Int. Ed.* **2002**, *41*, 1548. (b) Gaylord, B. S.; Heeger, A. J.; Bazan, G. C. *J. Am. Chem. Soc.* **2003**, *125*, 896. (c) Wang, S.; Bazan, G. C. *Adv. Mater.* **2003**, *15*, 1425. (d) Dwight, S. J.; Gaylord, B. S.; Hong, J. W.; Bazan, G. C. *J. Am. Chem. Soc.* **2004**, *126*, 16850.

(3) (a) Hoven, C. V.; Garcia, A.; Bazan, G. C.; Nguyen, T.-Q. *Adv. Mater.* **2008**, *20*, 3793. (b) Jiang, H.; Taranekar, P.; Reynolds, J. R.; Schanze, K. S. *Angew. Chem., Int. Ed.* **2009**, *48*, 4300.

(4) (a) Thomas, S. W. III; Joly, G. D.; Swager, T. M. *Chem. Rev.* **2007**, *107*, 1339. (b) Basabe-Desmonts, L.; Reinhoudt, D. N.; Crego-Calama, M. *Chem. Soc. Rev.* **2007**, *36*, 993. (c) Martínez-Máñez, R.; Sancenón, F. *Chem. Rev.* **2003**, *103*, 4419. (d) Kinami, M.; Crenshaw, B. R.; Weder, C. *Chem. Mater.* **2006**, *18*, 946.

(5) (a) Samuel, I. D. W.; Turnbull, G. A. *Chem. Rev.* **2007**, *107*, 1272. (b) McGehee, M. D.; Heeger, A. J. *Adv. Mater.* **2000**, *12*, 1655.

(6) (a) Hong, Y.; Lam, J. W. Y.; Tang, B. Z. *Chem. Commun.* **2009**, 4332. (b) Zeng, Q.; Li, Z.; Dong, Y.; Di, C.; Qin, A.; Hong, Y.; Ji, L.; Zhu, Z.; Jim, C. K. W.; Yu, G.; Li, Q.; Li, Z.; Liu, Y.; Qin, J.; Tang, B. Z. *Chem. Commun.* **2007**, 70. (c) An, B.-K.; Kwon, S.-K.; Jung, S.-D.; Park, S. Y. *J. Am. Chem. Soc.* **2002**, *124*, 14410. (d) Deans, R.; Kim, J.; Machacek, M. R.; Swager, T. M. *J. Am. Chem. Soc.* **2000**, *122*, 8565. (e) Hong, Y.; Lam, J. W. Y.; Tang, B. Z. *Chem. Soc. Rev.* **2011**, *40*, 5361.

(7) *Handbook of Liquid Crystals*; Demus, D., Goodby, J. W., Gray, G. W., Spiess, H.-W., Vill, V., Eds.; Wiley-VCH: Weinheim, 1998.

(8) (a) Kato, T.; Mizoshita, N.; Kishimoto, K. *Angew. Chem., Int. Ed.* **2006**, *45*, 38. (b) Sagara, Y.; Kato, T. *Nat. Chem.* **2009**, *1*, 605. (c) Kato, T. *Science* **2002**, *295*, 2414. (d) Pisula, W.; Feng, X.; Müllen, K. *Adv. Mater.* **2010**, *22*, 3634. (e) Kato, T.; Yasuda, T.; Kamikawa, Y.; Yoshio, M. *Chem. Commun.* **2009**, 729. (f) Kato, T.; Tanabe, K. *Chem. Lett.* **2009**, *38*, 634. (g) Donnio, B.; Bruce, D. W. *Struct. Bonding (Berlin)* **1999**, *95*, 193. (h) Saez, I. M.; Goodby, J. W. *Struct. Bonding (Berlin)* **2008**, *128*, 1. (i) Bushey, M. L.; Nguyen, T.-Q.; Zhang, W.; Horoszewski, D.; Nuckolls, C. *Angew. Chem., Int. Ed.* **2004**, *43*, 5446. (j) Palmans, A. R. A.; Meijer, E. W. *Angew. Chem., Int. Ed.* **2007**, *46*, 8948. (k) Gin, D. L.; Pecinovsky, C. S.; Bara, J. E.; Kerr, R. L. *Struct. Bonding (Berlin)* **2008**, *128*, 181. (l) Guillon, D. *Struct. Bonding (Berlin)* **1999**, *95*, 41. (m) van Nostrum, C. F.; Nolte, R. J. M. *Chem. Commun.* **1996**, 2385. (n) Rowan, S. J.; Mather, P. T. *Struct. Bonding (Berlin)* **2008**, *128*, 119. (o) Kikuchi, H. *Struct. Bonding (Berlin)* **2008**, *128*, 99. (p) Rosen, B. M.; Wilson, C. J.; Wilson, D. A.; Peterca, M.; Imam, M. R.; Percec, V. *Chem. Rev.* **2009**, *109*, 6275. (q) Bisoyi, H. K.; Kumar, S. *Chem. Soc. Rev.* **2011**, *40*, 306. (r) Lemieux, R. P. *Acc. Chem. Res.* **2001**, *34*, 845. (s) Kim, F. S.; Ren, G.; Jenekhe, S. A. *Chem. Mater.* **2011**, *23*, 682.

(9) (a) Binnemans, K. *Chem. Rev.* **2005**, *105*, 4148. (b) Bruce, D. W. *Acc. Chem. Res.* **2000**, *33*, 831. (c) Bazuin, C. G.; Guillon, D.; Skoulios, A.; Nicoud, J.-F. *Liq. Cryst.* **1986**, *1*, 181. (d) Ujiie, S.; Iimura, K. *Macromolecules* **1992**, *25*, 3174. (e) Haramoto, Y.; Akiyama, Y.; Segawa, R.; Ujiie, S.; Nanasawa, M. *J. Mater. Chem.* **1998**, *8*, 275. (f) Katoh, M.; Uehara, S.; Kohmoto, S.; Kishikawa, K. *Chem. Lett.* **2006**, *35*, 322.

(10) (a) Yoshio, M.; Ichikawa, T.; Shimura, H.; Kagata, T.; Hamasaki, A.; Mukai, T.; Ohno, H.; Kato, T. *Bull. Chem. Soc. Jpn.* **2007**, *80*, 1836. (b) Yoshio, M.; Mukai, T.; Ohno, H.; Kato, T. *J. Am. Chem. Soc.* **2004**, *126*, 994.

(11) (a) Yazaki, S.; Funahashi, M.; Kagimoto, J.; Ohno, H.; Kato, T. *J. Am. Chem. Soc.* **2010**, *132*, 7702. (b) Tanabe, K.; Kato, T. *Chem. Commun.* **2009**, 1864. (c) Yazaki, S.; Funahashi, M.; Kato, T. *J. Am. Chem. Soc.* **2008**, *130*, 13206. (d) Tanabe, K.; Yasuda, T.; Yoshio, M.; Kato, T. *Org. Lett.* **2007**, *9*, 4271.

(12) Markovitsi, D.; Lécuyer, I.; Clergeot, B.; Jallabert, C.; Strzelecka, H.; Veber, M. *Liq. Cryst.* **1989**, *6*, 83.

(13) (a) Haristoy, D.; Tsiourvas, D. *Chem. Mater.* **2003**, *15*, 2079. (b) Celso, F. L.; Pibiri, I.; Triolo, A.; Triolo, R.; Pace, A.; Buscemi, S.; Vivona, N. *J. Mater. Chem.* **2007**, *17*, 1201.

(14) (a) Boydston, A. J.; Pecinovsky, C. S.; Chao, S. T.; Bielawski, C. W. *J. Am. Chem. Soc.* **2007**, *129*, 14550. (b) Boydston, A. J.; Vu, P. D.; Dykhno, O. L.; Chang, V.; Wyatt, A. R. II; Stockett, A. S.; Ritschdorff, E. T.; Shear, J. B.; Bielawski, C. W. *J. Am. Chem. Soc.* **2008**, *130*, 3143.

(15) Giner, I.; Gascón, I.; Giménez, R.; Cea, P.; López, M. C.; Lafuente, C. *J. Phys. Chem. C* **2009**, *113*, 18827.

(16) (a) Olivier, J.-H.; Camerel, F.; Barberá, J.; Retailleau, P.; Ziessel, R. *Chem.-Eur. J.* **2009**, *15*, 8163. (b) Olivier, J.-H.; Camerel, F.; Ulrich, G.; Barberá, J.; Ziessel, R. *Chem.-Eur. J.* **2010**, *16*, 7134.

(17) (a) Grabowski, Z. W.; Rotkiewicz, K.; Rettig, W. *Chem. Rev.* **2003**, *103*, 3899. (b) Bhattacharyya, K.; Chowdhury, M. *Chem. Rev.* **1993**, *93*, 507. (c) Rettig, W. *Angew. Chem., Int. Ed. Engl.* **1986**, *25*, 971.

(18) (a) Röcker, C.; Heilemann, A.; Fromherz, P. *J. Phys. Chem.* **1996**, *100*, 12172. (b) Ephardt, H.; Fromherz, P. *J. Phys. Chem.* **1993**, *97*, 4540. (c) Fromherz, P.; Heilemann, A. *J. Phys. Chem.* **1992**, *96*, 6864. (d) Ephardt, H.; Fromherz, P. *J. Phys. Chem.* **1991**, *95*, 6792. (e) Ephardt, H.; Fromherz, P. *J. Phys. Chem.* **1989**, *93*, 7717.

(19) (a) Belcher, W. J.; Fabre, M.; Farhan, T.; Steed, J. W. *Org. Biomol. Chem.* **2006**, *4*, 781. (b) Turner, D. R.; Paterson, M. J.; Steed, J. W. *J. Org. Chem.* **2006**, *71*, 1598. (c) Wallace, K. J.; Belcher, W. J.; Turner, D. R.; Syed, K. F.; Steed, J. W. *J. Am. Chem. Soc.* **2003**, *125*, 9699. (d) Abouderbala, L. O.; Belcher, W. J.; Boutelle, M. G.; Cragg, P. J.; Dhaliwal, J.; Fabre, M.; Steed, J. W.; Turner, D. R.; Wallace, K. J. *Chem. Commun.* **2002**, 358.

(20) Tanabe, K.; Yasuda, T.; Kato, T. *Chem. Lett.* **2008**, *37*, 1208.

(21) (a) Kimura, M.; Hatano, T.; Yasuda, T.; Morita, J.; Akama, Y.; Minoura, K.; Shimomura, T.; Kato, T. *Chem. Lett.* **2009**, *38*, 800. (b) Isoda, K.; Yasuda, T.; Kato, T. *Chem. Asian J.* **2009**, *4*, 1619. (c) Hatano, T.; Kato, T. *Chem. Commun.* **2006**, 1277. (d) Stals, P. J. M.; Smulders, M. M. J.; Martín-Rapffln, R.; Palmans, A. R. A.; Meijer, E. W. *Chem.-Eur. J.* **2009**, *15*, 2071. (e) Lehmann, M.; Jahr, M.; Donnio, B.; Graf, R.; Gemming, S.; Popov, I. *Chem.-Eur. J.* **2008**, *14*, 3562. (f) Gómez-Lor, B.; Alonso, B.; Omenat, A.; Serrano, J. L. *Chem. Commun.* **2006**, 5012. (g) Palmans, A. R. A.; Vekemans, J. A. J. M.; Fischer, H.; Hikmet, R. A.; Meijer, E. W. *Chem.-Eur. J.* **1997**, *3*, 300. (h) Kobayashi, Y.; Matsunaga, Y. *Bull. Chem. Soc. Jpn.* **1987**, *60*, 3515. (i) Lehmann, M.; Jahr, M.; Grozema, F. C.; Abellon, R. D.; Siebbeles, L. D. A.; Müller, M. *Adv. Mater.* **2008**, *20*, 4414. (j) Hennrich, G.; Ortiz, P. D.; Cavero, E.; Hanes, R. E.; Serrano, J. L. *Eur. J. Org. Chem.* **2008**, 4575. (k) Yasuda, T.; Shimizu, T.; Liu, F.; Ungar, G.; Kato, T. *J. Am. Chem. Soc.* **2011**, *133*, 13437.

(22) Yasuda, T.; Ooi, H.; Morita, J.; Akama, Y.; Minoura, K.; Funahashi, M.; Shimomura, T.; Kato, T. *Adv. Mater.* **2009**, *19*, 411.

(23) Reichardt, C. *Chem. Rev.* **1994**, *94*, 2319.

(24) (a) Kawamura, Y.; Sasabe, H.; Adachi, C. *Jpn. J. Appl. Phys.* **2004**, *43*, 7729. (b) Katoh, R; Suzuki, K.; Furube, A.; Kotani, M.; Tokumaru, K. *J. Phys. Chem. C* **2009**, *113*, 2961. (c) Suzuki, K.; Kobayashi, A.; Kaneko, S.; Takehira, K.; Yoshihara, T.; Ishida, H.; Shiina, Y.; Oishi, S.; Tobita, S. *Phys. Chem. Chem. Phys.* **2009**, *11*, 9850. (d) Hasegawa, M.; Kunisaki, S.; Ohtsu, H.; Werner, F. *Monatsh. Chem.* **2009**, *140*, 751.
(25) Margolis, B. J.; Long, K. A.; Laird, D. L. T.; Ruble, J. C.; Pulley, S. R. *J. Org. Chem.* **2007**, *72*, 2232.
(26) Steinke, N.; Frey, W.; Baro, A.; Laschat, S.; Drees, C.; Nimtz, M.; Hägele, C.; Giesselmann, F. *Chem.-Eur. J.* **2006**, *12*, 1026.